Electronic Supplementary Information (ESI)

Environmental and economic assessment of lactic acid production from glycerol using cascade bio- and chemocatalysis

Merten Morales,‡ Pierre Y. Dapsens,‡ Isabella Giovinazzo, Julia Witte, Cecilia Mondelli*, Stavros Papadokonstantakis*, Konrad Hungerbühler and Javier Pérez-Ramírez*

Institute for Chemical and Bioengineering, Department of Chemistry and Applied Biosciences, ETH Zurich, Vladimir-Prelog-Weg 1, CH-8093 Zurich, Switzerland. Fax: +41 44 6331405 Tel: +41 44 6337120; E-mails: cecilia.mondelli@chem.ethz.ch; stavros.papadokonstantakis@chem.ethz.ch; jpr@chem.ethz.ch.

1. Experimental

1.1. Catalyst synthesis and characterisation

Sn-MFI was synthesised according to the method reported elsewhere.[1] TEOS (93.7 g, Sigma-Aldrich, 98%) was mixed with a solution of $SnCl_4 \cdot 5H_2O$ (1.26 g, Sigma-Aldrich, 98%) in deionised H_2O (30 g) and allowed to react for 30 min under stirring. Then, TPAOH (198 g, Alfa Aesar, 20 wt.%) was added drop-wise and the mixture was stirred for another hour. Finally, 84 g of deionised H_2O were added and the solution was stirred for 30 min. The final molar ratio of the synthesis gel was $0.008\ SnO_2$:1 SiO_2:0.44 $TPAOH$:34.3 H_2O. The gel was transferred into a 500-cm^3 Teflon-lined autoclave, which was heated in an oven at 433 K for 3.5 days under static conditions. The obtained solid was recovered by filtration, washed thoroughly with deionised water, dried overnight at 338 K and finally calcined in static air at 823 K (heating rate: 5 K min^{-1}) for 5 h to ensure the complete removal of the organic structure-directing agent.

HSZ890 H0A (silicalite-1) was used for post-synthetic alkaline-assisted stannation.[2] The latter consisted of an alkaline treatment (AT) in an aqueous 0.3 M NaOH solution (15 cm^3 per gram of dried zeolite) containing 0.04 M of $SnSO_4$ (Acros, 98%) at 338 K for 30 min in an Easymax™ 102 reactor (Mettler Toledo). Due to the low solubility of the tin hydroxide formed, the solution was heated at 318 K for 1 h and filtered to remove the precipitate prior to the addition of the zeolite. The resulting modified metallosilicate (denoted as MFI-ATSn) was converted into its protonic form by three consecutive ion exchanges in aqueous 0.1 M NH_4NO_3 (6 h, 298 K, 100 cm^3 per gram of dried zeolite) and calcined as described above.

The carbon content in the used catalysts was determined by elemental analysis using a LECO CHN-9000 instrument. The content of Si and Sn in the solids and in the reaction mixtures was determined by inductively coupled plasma optical emission spectroscopy (ICP-OES) using a Horiba Ultra 2 instrument equipped with a photomultiplier tube detector. Prior to the measurements, the materials were digested in an acidic mixture ($HCl/HNO_3/HF$) under heating (343 K, overnight). Nitrogen sorption at 77 K was performed using a Quantachrome Quadrasorb-SI analyser on degassed samples (10^{-1} mbar, 573 K, 3 h). Powder X-ray diffraction (XRD) was conducted in a PANalytical X'Pert PRO-MPD diffractometer. Data were recorded in the 5-70° 2θ range with an angular step size of 0.05° and a counting time of 7 s per step. Fourier transform infrared (FTIR) spectroscopy of adsorbed pyridine was performed in a Bruker IFS 66 spectrometer equipped with a liquid N_2-cooled MCT detector. Self-supporting zeolite wafers (5 tons cm^{-2}, 20 mg, 1 cm^2) were pretreated at 10^{-3} mbar and 693 K for 4 h. After cooling down to room temperature, the samples were saturated with pyridine vapour (Sigma-Aldrich, >99.9%) and then evacuated at room temperature for 15 min and subsequently at 473 K for 30 min. Spectra were recorded in the 4000-650 cm^{-1} range at 4 cm^{-1} resolution by co-addition of 32 scans.

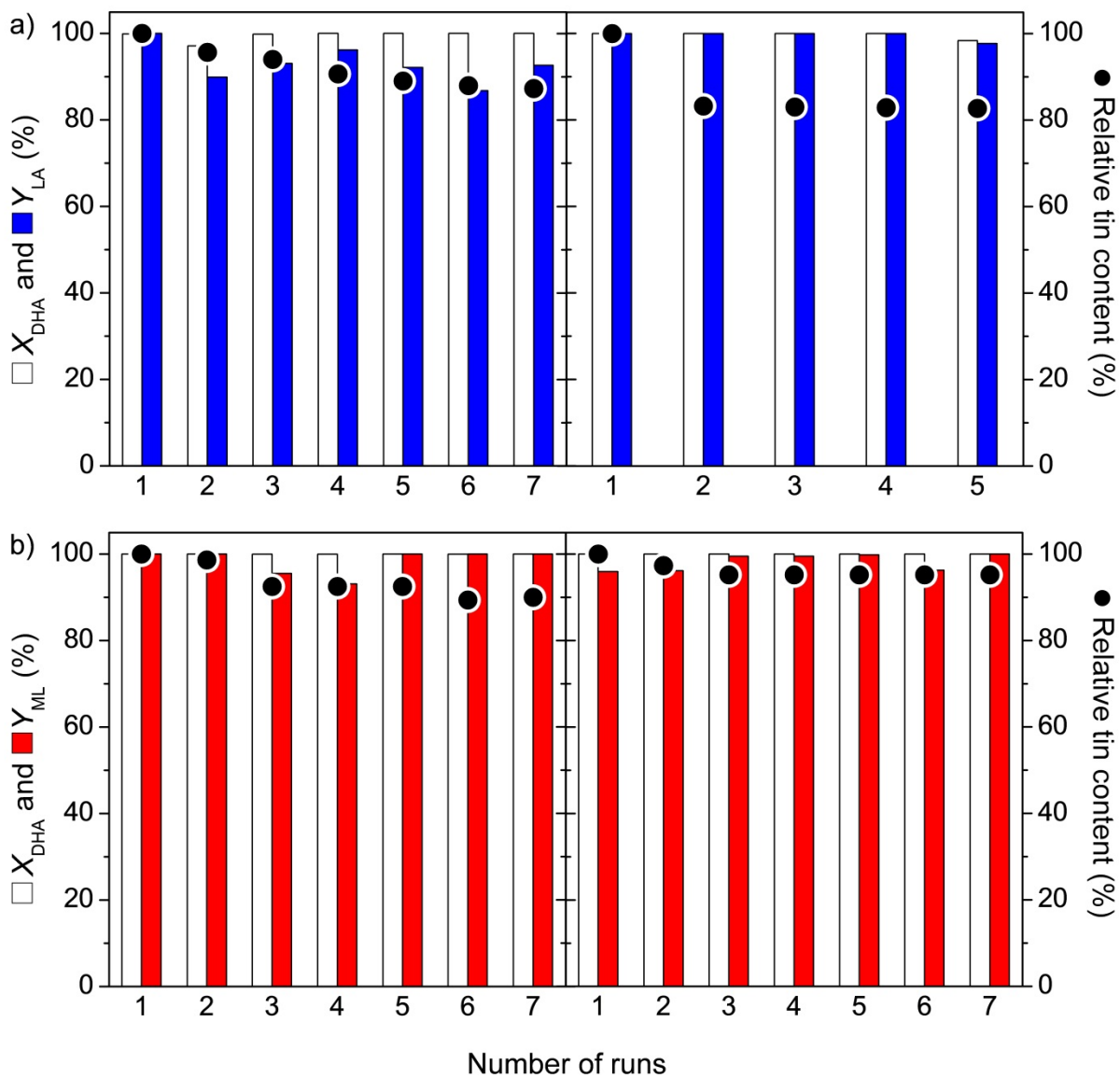## 1.2. Catalyst recyclability

Fig. S1 Recyclability tests of the Sn-MFI (left panel) and MFI-ATSn (right panel) catalysts in (a) water and (b) methanol. The solids were calcined (823 K, 5 K min^{-1}, 5 h) prior to every reuse in order to remove the adsorbed by-products.
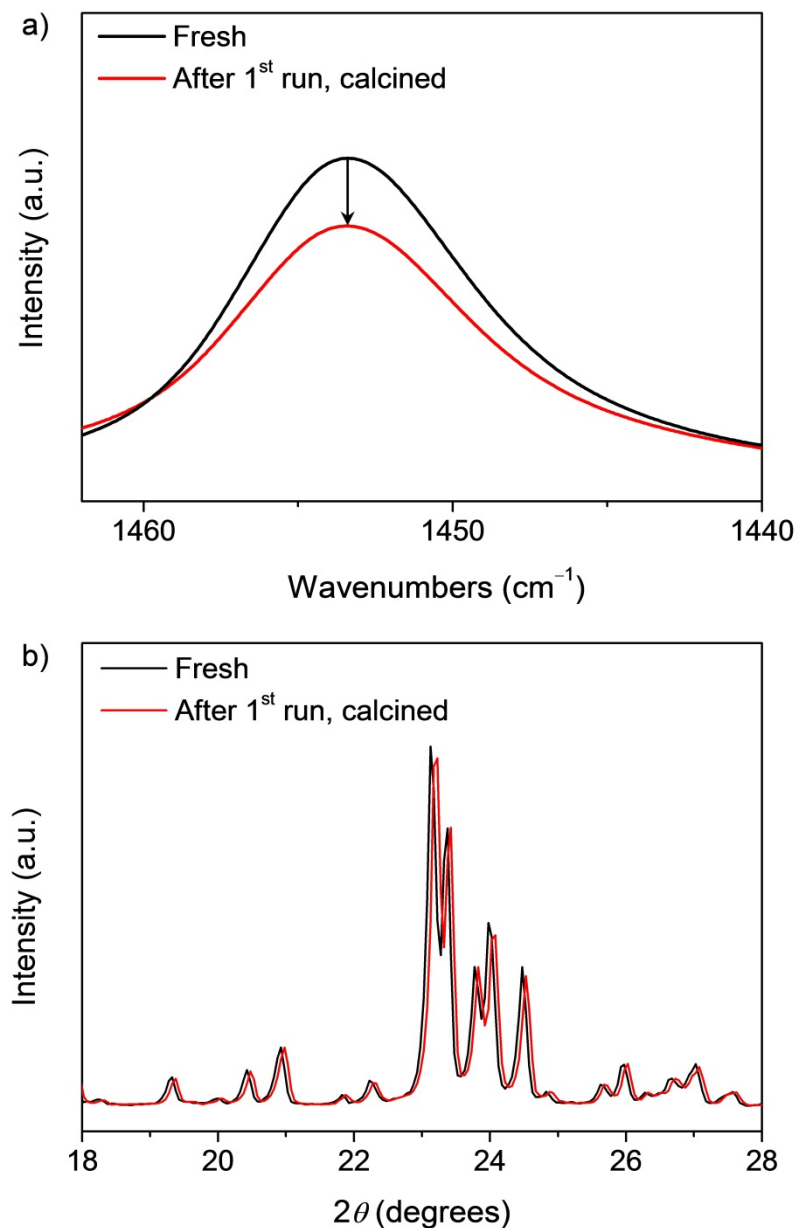
1.3. Catalyst characterisation

Fig. S2 (a) FTIR spectra of adsorbed pyridine and (b) XRD patterns of MFI-ATSn in fresh form and after one catalytic run in water. While the crystallinity of the zeolite was retained upon use, the concentration of Lewis-acid sites (calculated according to the method reported in [3]) decreased by 22%, which is in substantial agreement with the tin loss displayed in Fig. S1.

2. Process modelling

2.1. Biocatalytic LA production

The flowsheet generated for the conventional biocatalytic process for lactic acid (LA) production (*LA-5* model) is displayed in Fig. S3 and the relative life cycle inventory (LCI) data are shown in Table S1. The process comprises four main modelling steps: glucose (GLU) fermentation with *in situ* neutralisation of the as-formed LA with calcium hydroxide (Step-1), sulphuric acid-mediated hydrolysis of calcium lactate to LA (Step-2), esterification of LA to methyl lactate (ML) with recovery of the latter by distillation (Step-3) and hydrolysis of ML to recover pure LA (Step-4). Details to these steps are provided in the following.
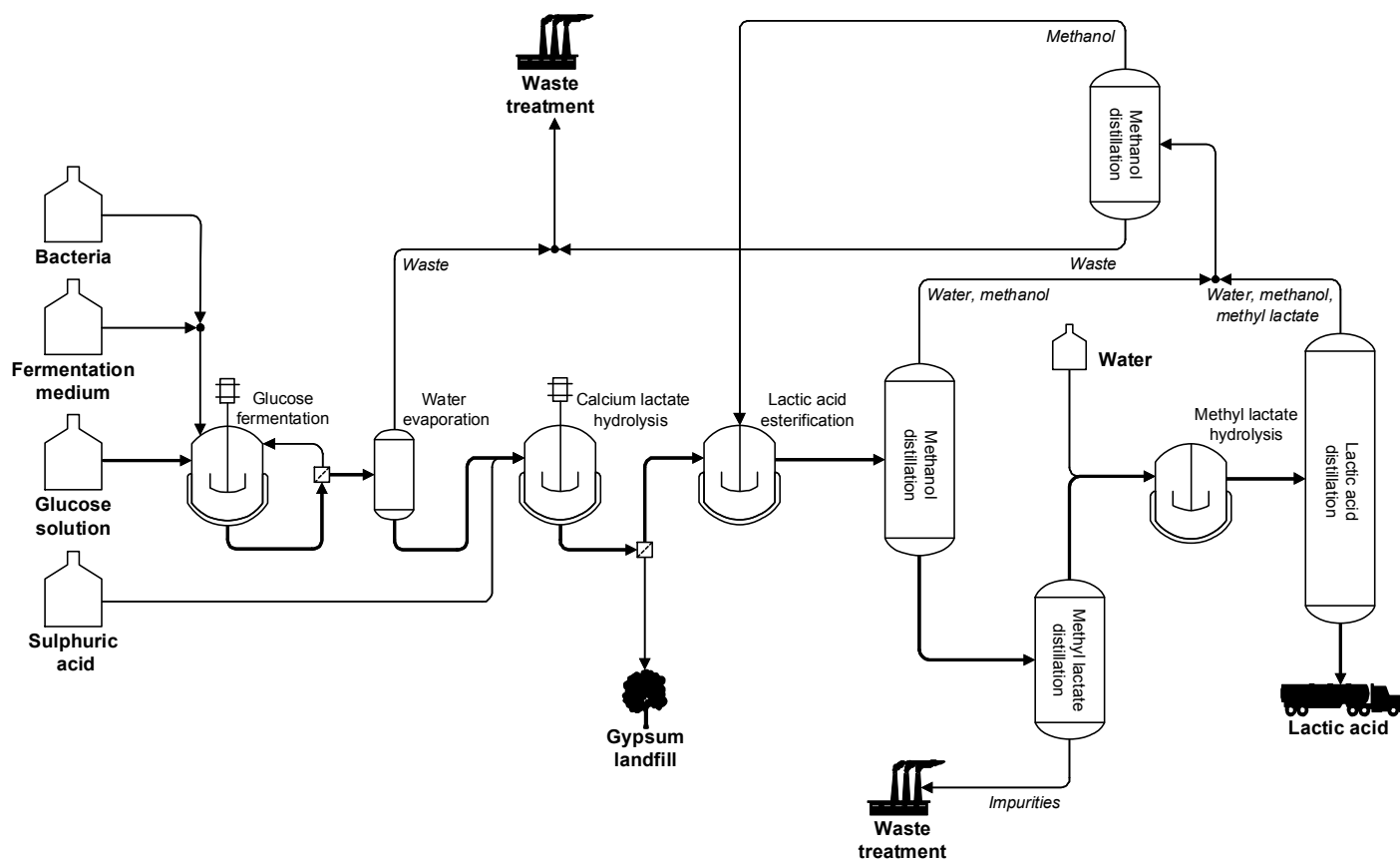

Fig. S3 Flowsheet for the LA production process from GLU according to the *LA-5* model.

Table S1 LCI data for the conventional biocatalytic LA production from GLU (*LA-5* model)

| Material and energy	*LA-5* model	Units
Glucose	1.52	kg kg$_{LA}^{-1}$
Process water	14.8	kg kg$_{LA}^{-1}$
H$_2$SO$_4$	1.48	kg kg$_{LA}^{-1}$
Methanol	0.02	kg kg$_{LA}^{-1}$
Bacteria	0.01	kg kg$_{LA}^{-1}$
Ca(OH)$_2$	0.76	kg kg$_{LA}^{-1}$
Nutrients	0.07	kg kg$_{LA}^{-1}$
Steam (6bar)	52.1	kg kg$_{LA}^{-1}$
Cooling water	107	kg kg$_{LA}^{-1}$
Waste	16.7	kg kg$_{LA}^{-1}$
Gypsum	0.95	kg kg$_{LA}^{-1}$

Step-1: GLU fermentation and in situ LA neutralisation

GLU fermentation and LA neutralisation were lumped in a single-step reaction:

$$C_6H_{12}O_6 + Ca(OH)_2 \longrightarrow [2(CH_3CHOCOO)^-]Ca^{2+} + 2H_2O$$

which was assumed to follow a pseudo power-law kinetics. The reaction was modelled using a RBATCH reactor in Aspen Plus® V8.2, considering a reaction time of 72 h, a temperature of 313 K, a pressure of 1 bar and a GLU conversion of 90%.[4] The input stream to the reactor had a composition of 84 wt.% water, 10 wt.% GLU, 5 wt.% calcium hydroxide and 1 wt.% nutrients. The LA bacteria (*lactobacillus*) content in the reactor was 4 wt.% with respect to the input stream.[5] Calcium hydroxide enabled to maintain the pH of the fermentation broth in the optimal range of 5.5-6.3 by converting LA to calcium lactate.[5,6]

Step-2: Sulphuric acid-mediated hydrolysis of calcium lactate

$$[2(CH_3CHOCOO)^-]Ca^{2+} + H_2SO_4 \longrightarrow 2CH_3CHOHCOOH + CaSO_4$$
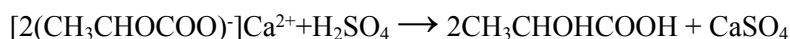
After flashing out most of the water, H_2SO_4 was injected (in an amount of twice the molar flow of calcium lactate) into the reactor to convert calcium lactate to LA by hydrolysis. This reaction was modelled with an RSTOIC reactor in Aspen Plus® V8.2, considering a reaction temperature of 403 K and a calcium lactate conversion of 90%.[7] A stoichiometric amount of $CaSO_4$ (*i.e.* gypsum) was formed in this transformation.[7] Owing to its relatively low solubility in water at 293 K (*ca.* 2.4 g L^{-1}),[8] it was assumed that 99 wt.% of the $CaSO_4$ can be separated through filtration. This gypsum is considered as a waste to be landfilled. This comprises the biggest disadvantage of the conventional LA production process.[9]

Step-3: Esterification of LA to ML and ML recovery by distillation

$$CH_3CHOHCOOH + CH_3OH \longrightarrow CH_3CHOHCOOCH_3 + H_2O$$
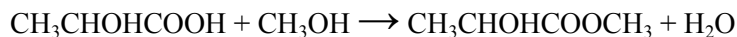
In order to separate LA from the other impurities formed in the fermentation process, an esterification with methanol was performed. In fact, thanks to the greater thermal stability of ML compared to LA, this avoids an energy-intensive and expensive vacuum distillation. This reaction was modelled with an RSTOIC reactor in Aspen Plus® V8.2, assuming a temperature of 353 K, a pressure of 1 bar, and a LA conversion of 88% and using a methanol input stream with 3 times the molar flow of that of LA.[10] After the esterification, water and methanol were first separated from ML, LA and impurities through distillation (DSTWU model in Aspen Plus® V8.2). In a second column (DSTWU model), ML was separated from impurities, which mainly comprised salts formed in the fermentation and LA that was not converted into ML. The waste stream of the second column was treated in a waste water treatment plant.

Noteworthily, the conversion of LA to ML is usually carried out in a reactive distillation column. A rigorous RADFRAC model in Aspen Plus® V8.2 for such a reactive distillation would require experimental data for the reaction rates, which are not available in the literature. Therefore, this modelling step was simplified considering an RSTOIC reactor model and a DSTWU distillation model in Aspen Plus® V8.2 in series.

Step-4: Hydrolysis of ML to LA

$$CH_3CHOHCOOCH_3 + H_2O \longrightarrow CH_3CHOHCOOH + CH_3OH$$
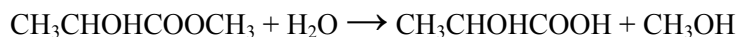
In this last step, ML was hydrolysed to LA in the presence of water and further purified by distillation. This reaction was modelled with a RSTOIC reactor in Aspen Plus® V8.2, considering a temperature of 353 K, assuming an ML

5

conversion of 95% and using a water input stream with 3 times the molar flow of ML.[7] LA was then separated from ML, water and methanol via a distillation column (DSTWU model in Aspen Plus® V8.2) operated at a pressure of 0.2 bar to ensure that the temperature of the reboiler does not exceed 453 K to prevent thermal degradation of LA. Under those conditions, LA was recovered with a purity of 99.99 wt.%.

Finally, methanol from Step-3 and Step-4 was recovered by distillation (DSTWU model) and recycled for the esterification of LA, whereas the outlet stream at the bottom of the column, containing mainly water, was directly sent to a waste water treatment plant.

## 2.2. Catalytic LA production from GLY-derived DHA

The alternative cascade process considered for the production of LA comprises the enzymatic conversion of glycerol (GLY) to DHA followed by its heterogeneously-catalysed isomerisation in water or isomerisation-esterification in methanol with subsequent hydrolysis. Environmental and economic aspects of this alternative route were studied, unravelling the impact of the type of solvent and the performance and recyclability of the catalyst used in DHA isomerisation. The latter comprised an alkaline-treated ZSM-5 zeolite,[11] denoted as MFI-AT, and the tin-containing MFI zeolites prepared by hydrothermal synthesis and alkaline-assisted stannation herein introduced, denoted as Sn-MFI and MFI-ATSn, respectively.

2.2.1. DHA production from GLY

For the DHA production from GLY, two process flowsheets were generated to account for the different purity of the GLY feedstock, which is either pure (99.99 wt.%, *DHA-1* model) or crude (various purities, see Table S6, *DHA-2* and *DHA-3* models).[12] The difference between the flowsheets is the presence of a pretreatment step for the removal of methanol, ash and matter organic non-glycerol (MONG) in the case of crude GLY to avoid potential GLY esterification in the DHA production steps. The flowsheet for the *DHA-2* and *DHA-3* models is shown in Fig. 1 of the main manuscript. This process can be divided into three main modelling steps: fermentation of GLY to DHA (Step-1), recovery of DHA through crystallisation out of butanol (Step-2) and recovery of butanol from the water-containing mother liquor through heterogeneous azeotropic distillation (Step-3). Details to these steps are provided below.

Step-1: Fermentation of GLY to DHA

The ash in the crude GLY was separated by conventional filtration (SSPLIT filter in Aspen Plus® V8.2). Since in 70% of the US biodiesel production sodium methylate represents the main constituent of the ash fraction, it was assumed that the ash only comprised this chemical species.[13] The crude GLY stream was then treated through flash evaporation (FLASH2 separator in Aspen Plus® V8.2) at 1 bar to remove most of the methanol and some of the water present. For the separation of MONG, a SEP separator in Aspen Plus® V8.2 could be applied. However, due to the lack of experimental data on the technology for the MONG separation from crude GLY, which is industrialised by PALL®,[14] this step was not modelled. The subsequent fermentation of GLY to DHA was modelled with an RBATCH reactor in Aspen Plus® V8.2, assuming a reaction time of 30 h, a temperature of 303 K, a pressure of 1 bar and a DHA conversion of 90%.[4] The input stream in the reactor had a composition of 89.5 wt.% water, 10 wt.%. GLY and 0.5 wt.% nutrients. The bacteria content in the reactor was 0.4 wt.% with respect to the input stream. Contrary to the fermentation of GLU to LA, no pH adjustment was required because the bacteria *gluconobacter oxydans* can stand pH values as low as 3.3.[15] GLY was completely converted into glyceric acid and DHA in a molar ratio of 0.028.[16] For the sake of simplicity, it was assumed that glyceric acid was the only by-product according to the following reaction scheme:

$$0.5O_2 + C_3H_8O_3 \longrightarrow C_3H_6O_3 + H_2O$$

$$O_2 + C_3H_8O_3 \longrightarrow C_3H_6O_4 + H_2O$$
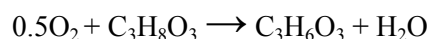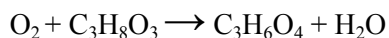
The fermentation broth was filtered and the bacteria were washed with water and recycled back into the fermenter. The liquid fraction was directed to the next flowsheet section for the recovery of DHA.

Step-2: Recovery of DHA through crystallisation out of butanol

The DHA recovery first comprised a flash evaporation (FLASH2 separator in Aspen Plus® V8.2) at 375 K and 1 bar for removing part of the water which is considered as a waste stream. Butanol was then added to the DHA-rich liquid stream in view of the relatively low solubility of DHA in this alcohol (*ca.* 6.3 g L^{-1} at 298 K) compared to water. After mixing, the stream was sent to a distillation column (DISTL column model in Aspen Plus® V8.2). In this separation step, a heterogeneous azeotropic mixture of water and butanol was removed from the top of the column while butanol with DHA and some glyceric acid impurities (< 1 wt.%) was recovered at the bottom of the column. The latter stream was treated in a crystalliser (CRYSTALLIZER solid model in Aspen Plus® V8.2) at 298 K where DHA precipitated. Glyceric acid remained in the mother liquor because its melting point is lower than 298K. DHA was separated from the mother liquor by filtration and directed to the LA production. The filtrate consisted of 95 wt.% butanol. Almost 99% of this butanol was recovered with a purity higher than 99.5 wt.% through a flash evaporation (FLASH2 separator in Aspen Plus® V8.2) that mainly removed the glyceric acid impurity. This was considered as a waste stream.

Along with the production of DHA to supply the LA manufacture, extra-pure DHA was produced for commercial use by implementing an additional unit in the process flowsheet. Thus, DHA was further washed (SWASH solid model in Aspen Plus® V8.2) with acetone and finally dried with air at 293 K (DRYER solid model in Aspen Plus® V8.2). The acetone stream leaving the washer was purified in a flash unit (FLASH2 separator in Aspen Plus® V8.2) and recycled (Fig. 1 in the main manuscript).

Step-3: Recovery of butanol from the water-containing mother liquor through heterogeneous azeotropic distillation

The heterogeneous butanol-water azeotrope (54 wt.% butanol and 46 wt.% water) was separated into an aqueous and an organic (*i.e.* butanol-rich) phase. The butanol-rich phase was recycled to the first column and the water-rich phase was directed to a second column. The remaining butanol was collected at the top of the latter unit in form of an azeotropic mixture, which was directed to a decanter while the resulting waste water was sent to a treatment plant. Almost all of the butanol could be recycled with this method of breaking the heterogeneous azeotrope. The make-up stream of fresh butanol was 0.61 kg h^{-1} and the butanol stream needed for the crystallisation 26.8 kg h^{-1}.

2.2.2. LA production from DHA in water

The DHA product stream was directed into the second part of the LA production, where DHA was converted into LA over zeolites. The flowsheet shown in Fig. S4 is based on the use of MFI-AT as the catalyst. Experimental data for this reaction have been presented elsewhere.[11] The flowsheet presented in Fig. 2a in the main manuscript considers tin-containing MFI catalysts, whose performance is reported in this paper. The structure of the two process flowsheets is similar. Firstly, DHA is converted into LA in a batch reactor (RBATCH reactor model in Aspen Plus® V8.2) and then LA is purified. LA production from DHA can be divided into three main modelling steps: the catalytic conversion of DHA into LA in water (Step-1), the recovery of the catalyst by filtration and regeneration *via* calcination (Step-2) and the separation of remaining impurities and DHA from LA by distillation and crystallisation with butanol in the model based on MFI-AT catalyst (Step-3a) or the recovery of LA through vacuum distillation in the model based on Sn-MFI catalyst (Step-3b). Details to these four steps are provided hereon.
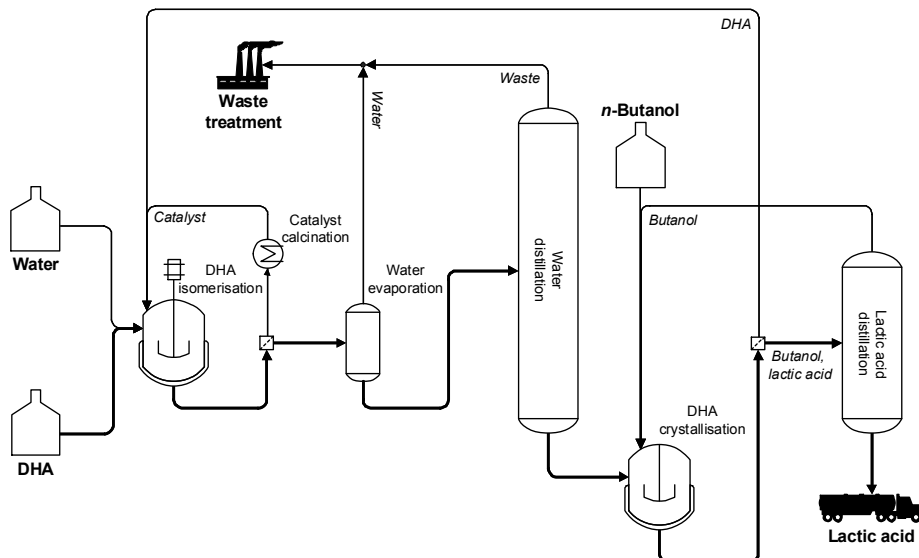
Fig. S4 Process flowsheet for the LA production from DHA with MFI-AT catalyst.

Step-1: Catalytic conversion of DHA to LA in water

In both flowsheets, the conversion of DHA into LA took place in a batch reactor modelled with an RBATCH model in Aspen Plus® V8.2. The inlet composition of the streams in the batch reactor is shown in Table S2 and the settings of the RBATCH model are summarised in Table S3.

Table S2 Composition of the mixture for the batch catalytic conversion of DHA into LA in water over the tin-free and the tin-containing catalyst
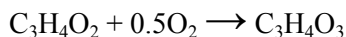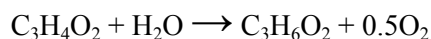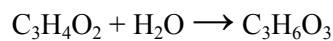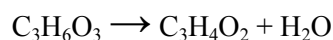
Inlet stream composition	MFI-AT model	Sn-MFI model	Units
DHA	15	15	wt.%
Catalyst	10	10	wt.%
Water	75	75	wt.%

Table S3 Settings for the batch reactor for the catalytic conversion of DHA into LA in water over the tin-free and the tin-containing catalyst

Reactor settings	MFI-AT model	Sn-MFI model	Units
Reaction time	6	1	h
Temperature	413	413	K
Pressure	4	4	bar
DHA conversion	90	100	%
LA yield	81	93	%
Catalyst recyclability	3	7	no. of runs

The DHA conversion and LA selectivity were 90 and 92% over MFI-AT[11] and 100 and 93% over Sn-MFI, respectively. Accordingly, a more energy-intensive purification of the outlet of the batch reactor was required in the first case. The Sn-MFI catalyst also exhibited a higher recyclability (7 runs) compared to the MFI-AT catalyst (3 runs).[11] While this parameter does not affects the purification steps, it leads to a larger catalyst consumption (the increased solid waste impact was not considered).

DHA was initially dehydrated into pyruvaldehyde, which was in turn transformed into LA, acetol and pyruvic acid. These steps are described by the following equations:

$$C_3H_6O_3 \longrightarrow C_3H_4O_2 + H_2O$$

$$C_3H_4O_2 + H_2O \longrightarrow C_3H_6O_3$$

$$C_3H_4O_2 + H_2O \longrightarrow C_3H_6O_2 + 0.5O_2$$

$$C_3H_4O_2 + 0.5O_2 \longrightarrow C_3H_4O_3$$

Step-2: Recovery of the catalyst by filtration and regeneration via calcination

The catalyst was separated from the reaction mixture by filtration and calcined at 823 K (5 K min⁻¹, 5 h) to remove the adsorbed by-products.

Step-3a: Recovery of LA through distillation and crystallisation (MFI-AT model)

After filtration, the stream was treated in a flash and a vacuum distillation unit (FLASH2 and DSTWU models in Aspen Plus® V8.2) to remove water and impurities. Thereafter, butanol was added to separate DHA from LA through crystallisation (CRYSTALLIZER model in Aspen Plus® V8.2) and filtration (SSPLIT model in Aspen Plus® V8.2). The DHA obtained was recycled back to the batch reactor. The LA-butanol mixture generated in this work-up was separated in a vacuum distillation unit (DSTWU model in Aspen Plus® V8.2).

Step-3b: Recovery of LA through distillation (Sn-MFI model)

The water content of the mixture was reduced by 60% using a flash evaporator operated at 375 K and 1 bar. The concentrated mixture underwent a vacuum distillation (DSTWU model in Aspen Plus® V8.2) which enabled to recover LA at the bottom of the column with a purity of 99.99 wt.% and water, acetol and pyruvic acid at the top of the column, which were sent to a waste water treatment plant. The column was operated at 0.04 bar to ensure that the temperature at the bottom of the column was below 453 K to prevent the thermal decomposition of LA.

2.2.3. LA production from DHA in methanol

In this case, DHA was isomerised in methanol to ML and LA was recovered by a subsequent hydrolysis step. The process flowsheet is shown in Fig. 2b in the main manuscript and can be divided into four main modelling steps: the catalytic conversion of DHA into ML in methanol (Step-1), the recovery of the catalyst by filtration and regeneration via calcination (Step-2), the recovery of LA through hydrolysis in a reactive distillation (Step-3) and the recovery of unreacted methanol by distillation (Step-4).

Step-1: Catalytic conversion of DHA to ML in methanol

The conversion of DHA to LA took place in a batch reactor (RBATCH model in Aspen Plus® V8.2). The inlet composition of the streams and the settings of the RBATCH model are shown in Tables S4 and S5, respectively.

Table S4 Batch reactor inlet composition for the catalytic conversion of DHA into LA in methanol over the tin-containing catalyst

Inlet stream composition	Sn-MFI model	Units
DHA	15	wt.%
Catalyst	10	wt.%
Methanol	75	wt.%

Table S5 Settings of the batch reactor for the catalytic conversion of DHA into LA in methanol over the tin-containing catalyst

Reactor settings	Sn-MFI model	Units
Batch time	2	h
Reactor temperature	413	K
Reactor pressure	11	bar
DHA conversion	100	%
ML yield	97	%
Catalyst recyclability	7	no. of runs

The experimental results for this reaction indicated that no by-product was formed. Thus, the reaction could be simply expressed as:
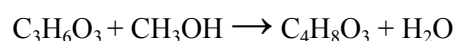
$$C_3H_6O_3 + CH_3OH \longrightarrow C_4H_8O_3 + H_2O$$

Step-2: Recovery of the catalyst by filtration and regeneration via calcination

The catalyst was separated from the reaction mixture by filtration and calcined at 823 K (5 K min^{-1}, 5 h) to remove the adsorbed by-products. The recyclability of the Sn-MFI catalyst was the same in the methanol and water environment, as shown in Tables S3 and S5.

Step-3: Recovery of LA through hydrolysis in a reactive distillation

The reaction mixture underwent a first distillation to separate ML from practically all the unreacted methanol (DSTWU model in Aspen Plus® V8.2). The ML leaving the bottom of the column is typically hydrolysed in a reactive distillation column. Due to the lack of experimental data and process information, this step was herein modelled combining an RSTOIC reactor and a DSTWU model in Aspen Plus® V8.2 in series. The reaction in RSTOIC took place at 353 K and 1 bar in the presence of added water. The molar ratio of ML to water in the inlet stream of the reactor was 1:3. The fractional conversion of ML was set to 0.95.[7] The mixture of methanol, ML, water and LA was directed to a distillation column, where practically all LA was recovered at the bottom with a purity of 99.99 wt.%. The column was operated at 0.1 bar to prevent the thermal decomposition of LA.

Step-4: Recovery of methanol

While all of the methanol present in the outlet stream of the batch reactor was recovered from the top of the first distillation column in Step-3 (purity 99.99 wt.%), further methanol was generated by the hydrolysis of ML (DSTWU model in Step-3) which needed to be recovered by separating it from water and traces of unhydrolised ML. This was performed in a distillation column (DSTWU model in Aspen Plus® V8.2) which enabled to obtain 99.9% of the methanol at a purity of 99.98 wt.%. The methanol recovered from both columns was recycled back to the batch reactor for the conversion of DHA into ML. The waste stream, leaving the bottom of this last column was sent to a waste water treatment plant.

3. Process assessment

The production of LA through the alternative cascade process from crude GLY was first evaluated using a standard GLY composition (Table S6) selected based on the study of Hansen *et al*.[12] In particular, this composition was calculated averaging the data reported for each fraction in Table 2 of the mentioned article, excluding the entry relative to a GLY feedstock of exceptionally low quality (*i.e.*, 38.4 wt.%). In addition, other three GLY compositions were

considered (Table S6). In the high ash and high methanol cases, the ash or methanol content was increased by an amount corresponding to the water fraction, which was simultaneously set to zero. Noteworthy, the depletion of the water content in these scenarios implies a higher resource consumption of process water, since the inlet concentration of GLY in the fermentation unit should not exceed 10 wt.%. Furthermore, while the lack of water would suggest a more convenient alternative disposal of the crude GLY in an incineration unit, our comparative situation remained the disposal in a waste water treatment plant. Indeed, the analysis of these non-realistic GLY compositions was only meant to unravel the impact of the purification of single components on the overall process sustainability, which was still contrasted to the most representative alternative disposal strategy. The low GLY composition was generated considering the GLY content in the feedstock neglected in the calculation of the standard composition, maintaining the water, ash and MONG contents of the standard case and defining an amount of methanol sufficient to close the balance to 100%.

Table S6 Inlet compositions of crude GLY considered in the study of the alternative cascade process

	Standard	High ash	High methanol	Low GLY	Units
GLY	75.84	75.84	75.84	38.40	wt.%
Water	5.98	0	0	5.98	wt.%
Ash	5.32	11.30	5.32	5.32	wt.%
Methanol	3.29	3.29	9.27	40.73	wt.%
MONG	9.57	9.57	9.57	9.57	wt.%

3.1. Standard GLY composition

3.1.1. Global warming potential

The global warming potential (GWP) values (Fig. S5) show similar trends to the CED results presented and discussed in the main manuscript. More specifically, the data indicate that the conventional process (*LA-5* model) emits into the environment 7.6 kg of CO_2 per kg of LA. For the alternative process, the highest environmental burden is the production of DHA from pure GLY. Indeed, the GWP for the *DHA-1* model alone is 7.1 kg_{CO2-eq} kg_{DHA}^{-1}. The production of DHA from crude GLY has at least a 30% lower impact than its production from pure GLY if the alternative utilisation scenario for GLY is burning in an incineration plant, recovering the respective steam and/or electricity (*DHA-2* model). If crude GLY is considered as a waste to be treated in a waste water treatment plant, the
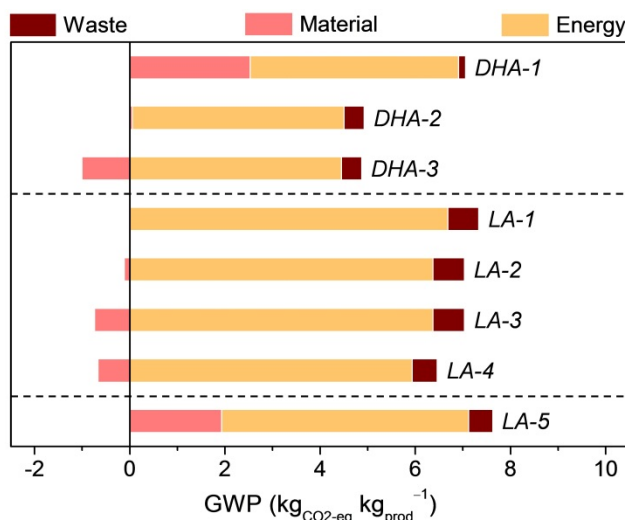

Fig. S5 Cradle-to-gate LCA according to the GWP-100a metric for various process scenarios.

GWP value becomes even smaller (3.9 kg_{CO2-eq} kg_{DHA}^{-1}, *DHA-2* model). The cascade LA production process using the MFI-AT catalyst (*LA-1* model) has a GWP value of 7.3 kg_{CO2-eq} kg_{LA}^{-1}. When the Sn-MFI catalyst is employed (*LA-2* model), the environmental impact is reduced to 6.9 kg_{CO2-eq} kg_{LA}^{-1} since the full DHA conversion and extremely high LA selectivity in this case enable a less energy-intensive purification of the LA stream. The lowest environmental impact (5.8 kg_{CO2-eq} kg_{LA}^{-1}) can be reached when the conversion of DHA into LA is performed in methanol (*LA-4* model). In this best-case scenario, the improvement of the GWP value is 24% compared to the conventional method (*LA-5* model).

3.1.2. Eco-Indicator 99

The trends of the Eco-Indicator 99 (EI99) values (Fig. S6) are similar to the CED and GWP cases, although larger variations are observed. In particular, the results show that the conventional design (*LA-5* model) has an environmental impact of 0.53 points kg_{LA}^{-1}. In relation to the DHA production from GLY, the environmental impact is the highest if pure GLY is used (1.09 points kg_{DHA}^{-1}, *DHA-1* model), because of the strong contribution of this feedstock to the material impact. This value can be reduced to 0.38 or 0.26 points kg_{DHA}^{-1} if crude GLY is considered as a waste to be treated in an incineration or waste water treatment plant, respectively. Accordingly, a decrease of the environmental footprint of even 65% can be determined for the biocatalytic step of the DHA production. The cascade *LA-4* process leads to an environmental impact for LA production of 0.39 points kg_{LA}^{-1}, which represents a reduction of 26% compared to the conventional technology (*LA-5* model). The impact of the materials on the LA production according to the EI99 indicator is not negative as in the case of the GWP metric (Fig. S5). The reason is that the catalyst has a higher impact for the EI99 compared to the GWP indicator.
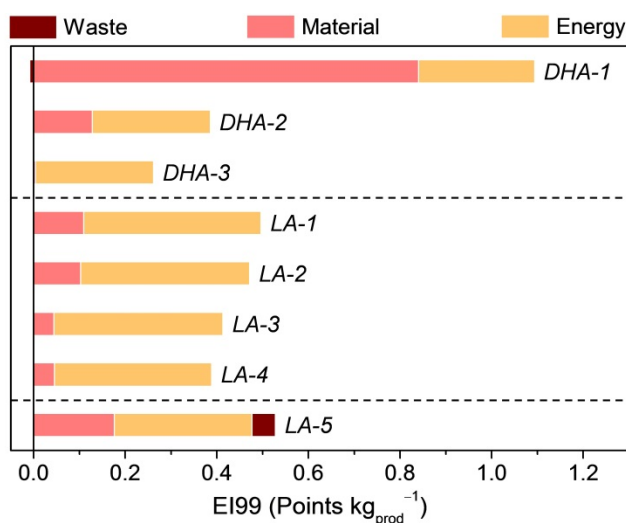

Fig. S6 Cradle-to-gate LCA according to the EI99 metric for various process scenarios.

3.1.3. Economic assessment

The results of the economic assessment are shown in Fig. S7. The currently practiced GLU fermentation process (*LA-5* model) gives a profit of only 0.04 USD kg_{LA}^{-1} due to the high operating costs. The highest profit with respect to GLY utilisation would be reached if DHA was considered as the end-product. For instance, assuming the *DHA-3* model, no competition for the utilisation of GLY with other markets (*i.e.* crude GLY is considered as a waste) and a market price of DHA of 4700 USD ton^{-1}[17], a profit of 3.8 USD kg_{LA}^{-1} could be obtained. Still, it has to be kept in mind that the market for DHA is rather small and easy to saturate,[17] Indeed, one strong motivation for its further processing to LA
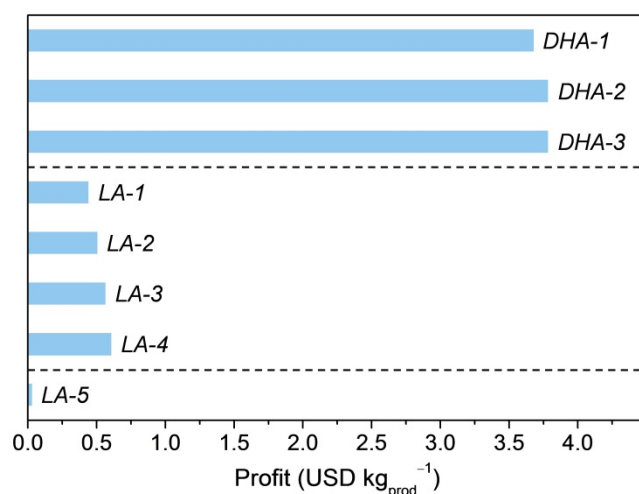
Fig. S7 Profit for various process scenarios.

is the much bigger market of the latter. The *LA-4* model has the highest profit (0.6 USD kg_{LA}), which is 15 times greater than for the current enzymatic route. All profit calculations mentioned above did not include the respective investment expenditure.

3.2. Other GLY compositions

3.2.1. Cumulative energy demand

The CED values determined for the alternative processes using GLY with non-standard composition are depicted in Fig. S8. Due to the low additional energy input for the purification of the GLY feedstock and for the waste water treatment, only a minor effect on the overall environmental impact was observed for the high ash and high methanol scenarios. A stronger variation was found for the low GLY case. Indeed, while the high concentration of methanol of this crude feedstock negligibly affects the energy required in the process, it leads to a more demanding waste treatment. Still, since the use of crude GLY as a chemical feedstock enables to save equivalent materials and energy input by avoiding its disposal, the overall CED values for the low GLY scenario remain very close to those determined for the standard GLY composition scenario. This outcome makes us confident that the non-quantifiable impact due to the MONG removal shall not compromise the meaningfulness of our analysis. The results of the assessment of the *LA-4* process using standard and low-quality GLY are detailed in Table S7.

Table S7 Cradle-to-gate LCA according to the non-renewable CED metric for the *LA-4* process scenarios based on the standard and low crude GLY compositions

	Standard	Low GLY	Units
Material	1.45	-19.34	$MJ_{eq}\ kg_{prod}^{-1}$
Energy	93.12	97.82	$MJ_{eq}\ kg_{prod}^{-1}$
Waste	1.57	22.31	$MJ_{eq}\ kg_{prod}^{-1}$
Total	96.13	100.79	$MJ_{eq}\ kg_{prod}^{-1}$

Fig. S8 Cradle-to-gate LCA according to the non-renewable CED metric for the (a) high ash, (b) high methanol and (c) low GLY scenarios.

3.2.2. Global warming potential

The trends in the GWP values for the high ash and high methanol scenarios resemble those of the CED values. In the low GLY case, the waste determines a strong increase in the environmental footprint but this is counterbalanced by the reduced impact of the materials which is due to the utilisation of waste GLY as a raw material.

Fig. S9 Cradle-to-gate LCA according to the non-renewable GWP metric for the (a) high ash, (b) high methanol and (c) low GLY scenarios.

3.2.3. Eco-Indicator 99

The process assessment results according to the EI99 metric are in line with those based on the CED and GWP indicators for the high ash and high methanol cases. For the low GLY scenario, the impact for the material in *LA-3* and *LA-4* vanishes. This is an effect of the reduced influence of the catalyst due to its high recyclability in these processes.
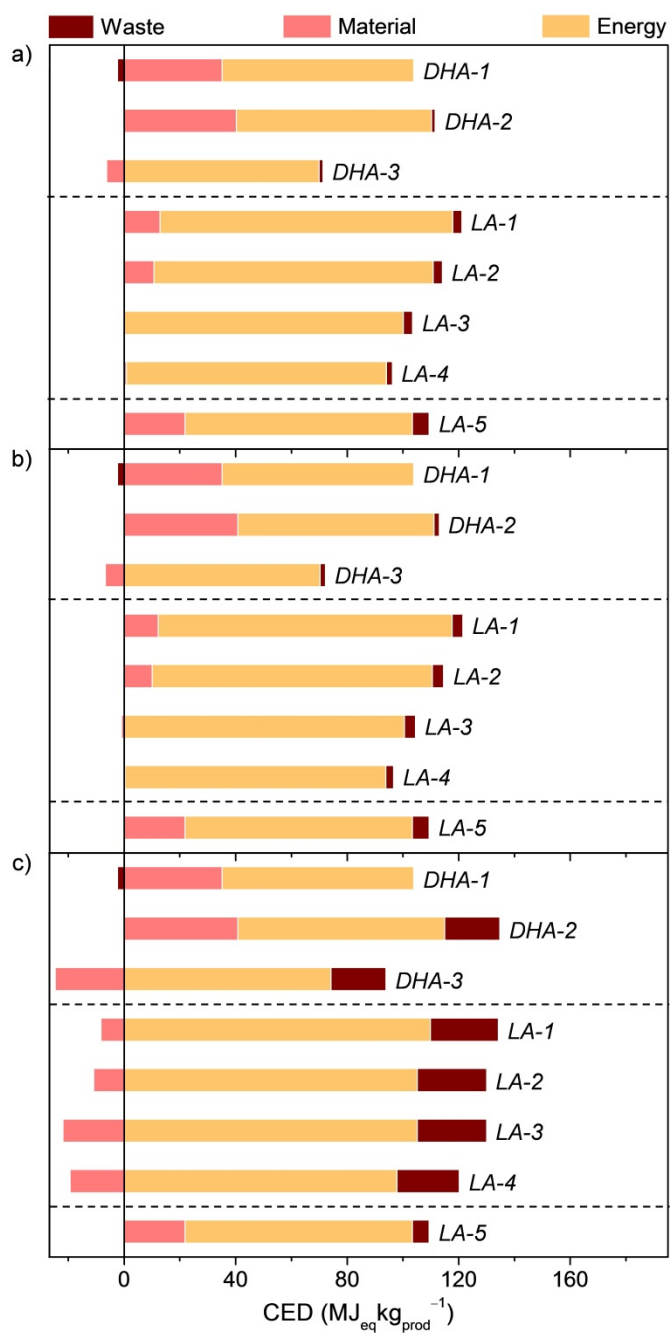

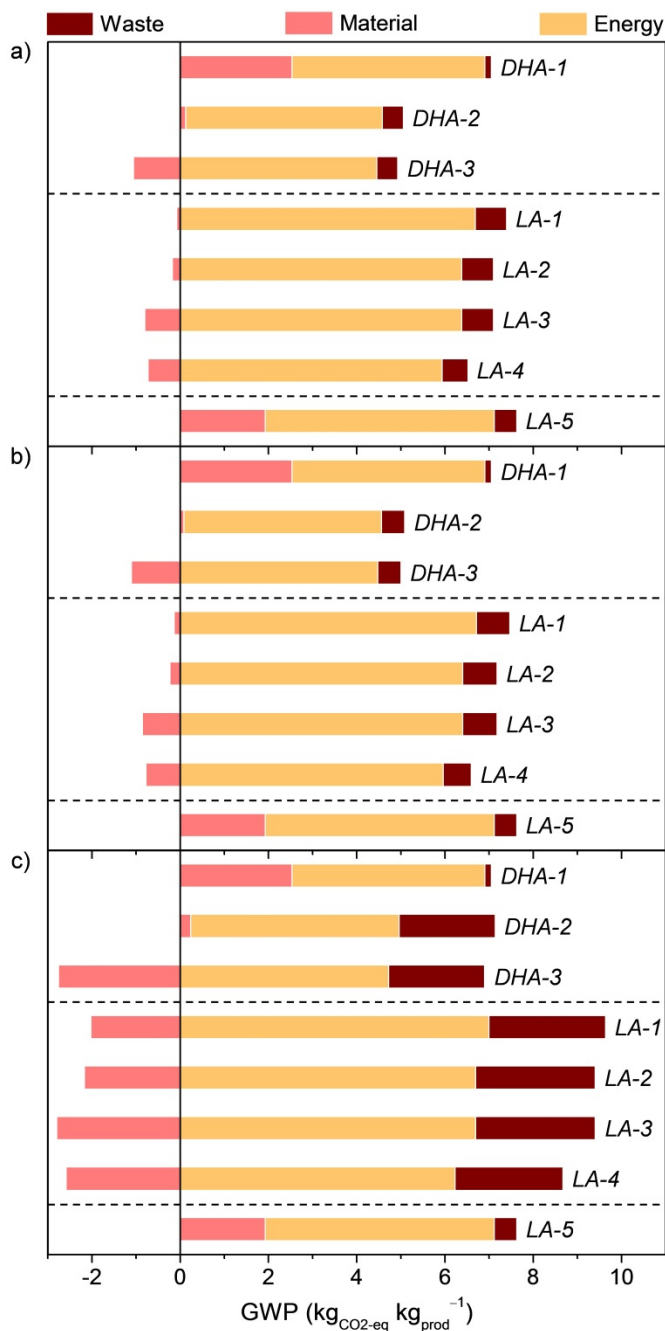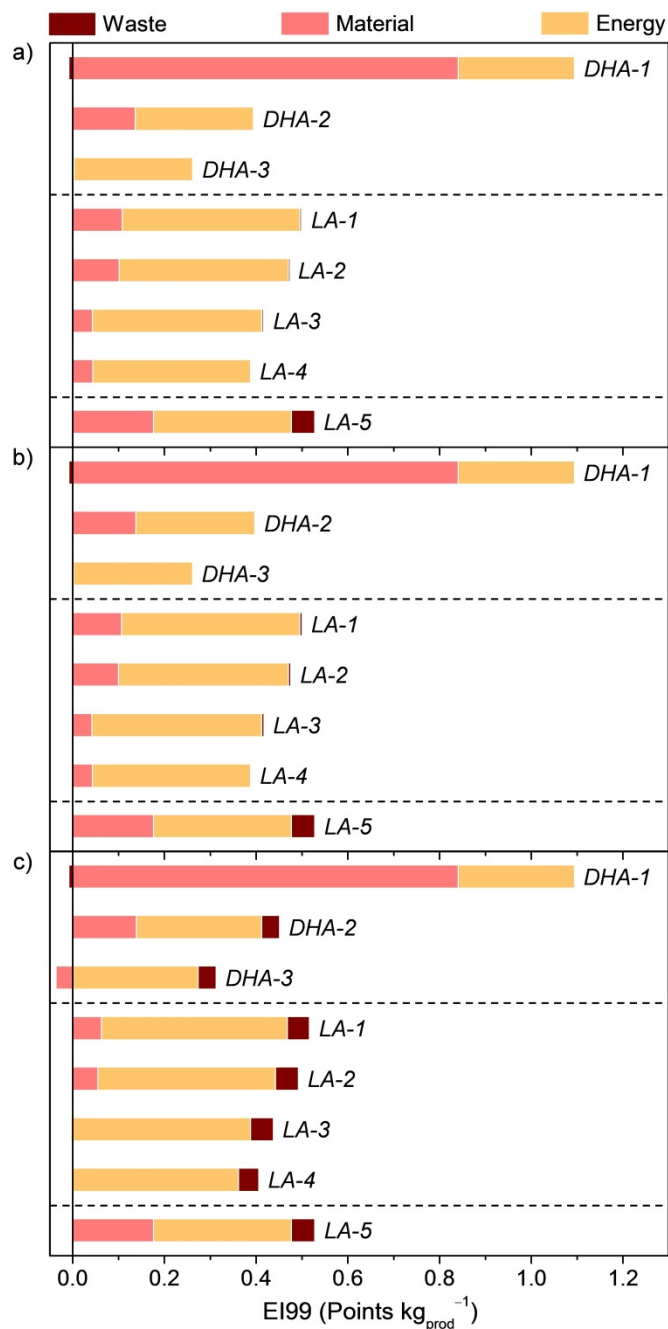**Fig. S10** Cradle-to-gate LCA according to the non-renewable EI99 metric for the (a) high ash, (b) high methanol and (c) low GLY scenarios.

3.2.4. Economic assessments

The results for the economic assessment of the processes using non-standard GLY compositions are shown in Fig. S11. Only minor variations in operating costs and profit compared to the standard scenario are detected for the high ash and high methanol situations. This is a consequence of a limited increase in the costs associated with the raw material pretreatment and the process waste treatment. In contrast, the use of a low-quality feedstock (low GLY case) leads to a significant increase in operating costs (36% for the *LA-4* model) since, due to the low concentration of GLY, a higher amount of crude GLY needs to be purchased to match the LA production in the standard scenario and a higher amount of methanol has to be treated in a waste water treatment plant. Still, it should be underlined that even in this case the profit of the alternative cascade process *LA-4* is 5 times higher than that of the conventional technology *LA-5*. Since it was assumed that the price of crude GLY does not to depend on its composition, but a low-purity GLY will realistically have a lower price, the profit of the alternative process might remain more considerable even when a low-quality GLY feedstock is employed.
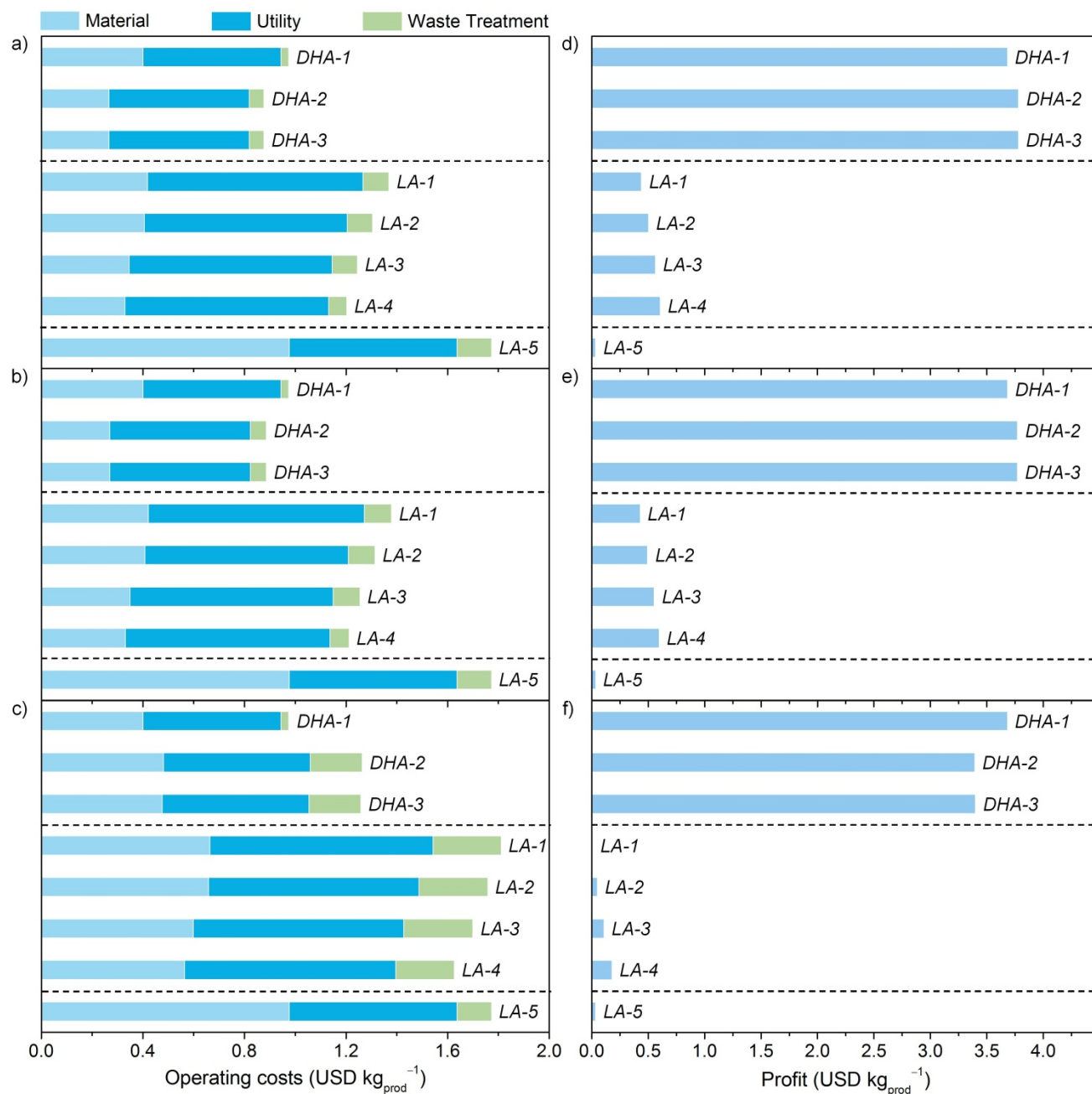
Fig. S11 Operating costs for the (a) high ash, (b) high methanol and (c) low GLY scenarios. Profit for the (d) high ash, (e) high methanol and (f) low GLY scenarios.

3.3. Background data for the environmental and economic assessment

The background data used in this study for the environmental and economic assessment with respect to the consumption of resources are presented in Table S8, while those related to the environmental impact of the process emissions (*i.e.,* those generated by the incineration units or waste water treatment plants, as no other direct process emissions are considered in this study) are presented in Table S9.

Table S8 Background data for the environmental (without renewable resources) and economic assessment with respect to resources consumption (Source: Ecoinvent database, www.alibaba.com and refs. [17,18])

Substance	CED (MJ_{eq} kg^{-1})	EI99 (Points kg^{-1})	GWP (kg_{CO2-eq} kg^{-1})	Price (USD ton^{-1})
Process water	2.79e-04	1.83e-06	2.45e-05	1
Ammonium sulphate	44.4	0.21	2.69	160
Diammonium phosphate	56.4	0.28	2.80	800
Glucose from sugar beet	6.49	0.05	0.51	400
Sulphuric acid	2.02	0.04	0.12	150
Methanol	37.4	0.13	0.74	348
Calcium hydroxide	5.50	0.03	0.99	100
Bacteria	18.6	0.08	1.04	1000
GLY	23.9	0.73	1.99	270
Butanol	80.4	0.29	2.60	822
Acetone	46.2	0.17	1.18	685
Zeolites	73.7	0.39	4.20	400
Crude GLY - INC	-18.3	-0.06	0.32	111
Crude GLY - WWTP	113	0.24	10.4	111
Steam (6bar)	1.56	0.01	0.10	20
Electricity (MU kWh^{-1})	9.87	0.02	0.49	0.10
Cooling water from river	0.00	0.00	0.00	0.15
Natural gas	1.24	4.03e-03	1.22e-02	600
Sodium hydroxide 30 wt.%	22.8	6.26e-02	1.09	570
Hydrochloric acid 32 wt.%	17.5	0.060	0.853	190
Polydimethylsiloxane	62.7	0.22	2.71	1000
Iron(III) chloride 40 wt.%	16.3	6.35e-02	0.803	360
Calcium chloride	11.0	5.18e-02	0.854	440
Gypsum landfill	0.65	4.22e-02	1.34e-02	4.81e-05

Table S9 Background data for the environmental impact for the emissions (Source: Ecoinvent database and ref. [18])[a]

Substance	EI99 (Points kg^{-1})	GWP (kg_{CO2-eq} kg^{-1})
Carbon dioxide	5.46e-02	1
Carbon monoxide	8.36e-02	-
Nitrogen dioxide	2.75	1.57
Particles	9.74	-
Ammonia	3.42	-

[a] Gypsum emissions are presented in Table S6.

3.4 Calculation of the environmental indicators

The LCA calculations for the flowsheets were performed based on the background data collected in Tables S8 and S9. Tables S10 and S11 show the calculations for LA production according to the conventional technology (*LA-5* model) and the most promising alternative cascade process (*LA-4* model) applying the standard crude GLY composition.

	Material								Energy			Waste	
	Water	Sulphate	Phosphate	Glucose	Sulphuric acid	Methanol	Calcium hydroxide	Bacteria	Steam (6bar)	Cooling water	Electricity	WWTP	Gypsum landfill
Flow (kg h^{-1})	166	0.42	0.42	17	17	0.25	8.45	0.13	585	12036	1.10E-03 [a]	188	10.63
CED (MJ$_{eq}$ h^{-1})[b]	0.05	18	24	111	33	9.35	46	2.42	914	0	1.09E-02	60	6.94
EI99 (Points h^{-1})[b]	0	0.09	0.12	0.86	0.64	0.03	0.22	0.01	3.37	0	2.52E-05	0.13	0.45
GWP (kg$_{CO2eq}$ h^{-1})[b]	0	1.13	1.18	8.65	2.01	0.19	8.33	0.14	58	0	5.36E-04	5.55	0.14
$\sum$CED (MJ$_{eq}$ h^{-1})[c]	245								915			67	
$\sum$EI99 (Points h^{-1})[c]	1.97								3.37			0.58	
$\sum$GWP (kg$_{CO2eq}$ h^{-1})[c]	22								58			5.69	
CED (MJ$_{eq}$ kg^{-1})[d]	21.83								81.52			5.99	
EI99 (Points kg^{-1})[d]	0.18								0.30			0.05	
GWP (kg$_{CO2eq}$ kg^{-1})[d]	1.93								5.19			0.51	
CED$_{Process}$ (MJ$_{eq}$ kg^{-1})[e]					109								
EI99$_{Process}$ (Points kg^{-1})[e]					0.53								
GWP$_{Process}$ (kg$_{CO2-eq}$ kg^{-1})[e]					7.63								

[a] Flow (kW)

[b] Obtained by multiplying the flow with the background data in Tables S8 and S9

[c] Summation of CED/EI99/GWP values for material, energy and waste

[d] Summation of CED/EI99/GWP values for material, energy and waste divided by the LA productivity calculated for this process (11.22 kg h^{-1})

[e] Summation of CED/EI99/GWP values of material, energy and waste

Table S10 LCA calculations for LA production *via* the conventional process

	Material								Energy			Waste	
	Water	Crude GLY	Sulphate	Phosphate	Butanol	Zeolites	Bacteria	Methanol	Steam (6bar)	Cooling Water	Electricity	WWTP	INC
Flow (kg h^{-1})	102	12.87	0.27	0.27	0.61	0.92	0.01	0.27	527	13672	0	108	1.26
CED (MJ$_{eq}$ h^{-1})^b	0.03	-115	11.93	15.11	49.29	68	0.15	10.19	823.62	0	0	18.59	-31
EI99 (Points h^{-1})^b	0	-0.25	0.06	0.08	0.18	0.36	0	0.03	3.04	0	0	0.04	-0.1
GWP (kg$_{CO2eq}$ h^{-1})^b	0	-10.64	0.72	0.75	1.59	3.87	0.01	0.20	52	0	0	1.71	0.55
$\sum$CED (MJ$_{eq}$ h^{-1})^c	39.09								823			-12.40	
$\sum$EI99 (Points h^{-1})^c	0.46								3.04			-0.06	
$\sum$ GWP (kg$_{CO2eq}$ h^{-1})^c	-3.50								52.47			2.26	
CED (MJ$_{eq}$ kg^{-1})^d	4.42								93.05			-1.40	
EI99 (Points kg^{-1})^d	0.05								0.34			-0.01	
GWP (kg$_{CO2eq}$ kg^{-1})^d	-0.40								5.93			0.26	
CED$_{Process}$ (MJ$_{eq}$ kg^{-1})^e				96									
EI99$_{Process}$ (Points kg^{-1})^e				0.39									
GWP$_{Process}$ (kg$_{CO2-eq}$ kg^{-1})^e				5.79									

^{a} Flow (kW)

^{b} Obtained by multiplying the flow with the background data in Tables S8 and S9

^{c} Summation of CED/EI99/GWP values for material, energy and waste

^{d} Summation of CED/EI99/GWP values for material, energy and waste divided by the LA productivity calculated for this process (8.85 kg h^{-1})

^{e} Summation of CED/EI99/GWP values of material, energy and waste

Table S11 LCA calculations for LA production from crude GLY *via* the alternative cascade *LA-4* process

References

[1]   N. K. Mal, V. Ramaswamy, P. R. Rajamohanan and A. V. Ramaswamy, *Microporous Mater.*, 1997, **12**, 331.

[2]   P. Y. Dapsens, C. Mondelli, B. T. Kusema, R. Verel and J. Pérez-Ramírez, *Green Chem.*, 2014, **16**, 1176.

[3]   C. A. Emeis, *J. Catal.*, 1993, **141**, 347.

[4]   R. Datta and M. Henry, *J. Chem. Technol. Biotechnol.*, 2006, **81**, 1119.

[5]   P. Dey, J. Sikder, S. Roy and P. Pal, *Clean Technol. Environ. Policy*, 2012, **14**, 827.

[6]   N. Thongchul, in *Bioprocessing Technologies in Biorefinery for Sustainable Production of Fuels, Chemicals, and Polymers,* S.-T. Yang, H. A. El-Henshay and N. Thongchul Eds., John Wiley and Sons, New Jersey, 2013, Chapter 16, p. 293.

[7]   M. Cockrem and P. Johnson, *US Patent* 5210296, 1993.

[8]   Available at www.echa.europa.eu, retrieved on 24.06.2014.

[9]   S. C. Prescott and C. G. Dunn, *Industrial Microbiology*, McGraw Hill, New York, 1959, p. 304.

[10]   X. Sun, Q. Wang, W. Zhao, H. Ma and K. Sakata, *Sep. Purif. Technol.*, 2006, **49**, 43.

[11]   P. Y. Dapsens, C. Mondelli and J. Pérez-Ramírez, *ChemSusChem*, 2013, **6**, 831.

[12]   C. F. Hansen, A. Hernandez, B. P. Mullan, K. Moore, M. Trezona-Murray, R. H. Kingand and J. R. Pluske, *Anim. Prod. Sci.*, 2009, **49**, 154.

[13]   P. Thane, *biofuels international*, 2008, **2**, 53

[14]   Available at www.pall.com/pdfs/Fuels-and.../FCBIODEN.pdf, Retrieved at October 2014

[15]   W. Charney, *US Patent* 4076589, 1987.

[16]   J. Svitel and E. Sturdik, *J. Ferment. Bioeng.*, 1994, **87**, 351.

[17]   A. Bridgwater, R. Chinthappali and P. Smith, *Identification and market analysis of most promising added-value products to be co-produced with the fuels*, Aston University, 2010.

[18]   C. Rerat, S. Papadokonstantakis and K. Hungerbühler, *J. Air Waste Manage. Assoc.*, 2013, 349.